Volume 5
Number 15
7 August 2023
Pages 3773–4004

Nanoscale Advances

rsc.li/nanoscale-advances

ISSN 2516-0230

ROYAL SOCIETY OF CHEMISTRY

COMMUNICATION

Riku Kawasaki, Atsushi Ikeda *et al.*

HER-2-targeted boron neutron capture therapy using an antibody-conjugated boron nitride nanotube/β-1,3-glucan complex

NCNST

Nanoscale Advances

ROYAL SOCIETY OF CHEMISTRY

COMMUNICATION

View Article Online
View Journal | View Issue

Cite this: *Nanoscale Adv.*, 2023, **5**, 3857

Received 13th January 2023
Accepted 23rd May 2023

DOI: 10.1039/d3na00028a

rsc.li/nanoscale-advances

HER-2-targeted boron neutron capture therapy using an antibody-conjugated boron nitride nanotube/β-1,3-glucan complex†

Keita Yamana,‡[a] Riku Kawasaki, ‡*[a] Kousuke Kondo,‡[a] Hidetoshi Hirano,[a] Shogo Kawamura,[a] Yu Sanada,[b] Kaori Bando,[c] Anri Tabata,[c] Hideki Azuma,[c] Takushi Takata,[b] Yoshinori Sakurai,[b] Hiroki Tanaka,[b] Tomoki Kodama,[d] Seiji Kawamoto,[d] Takeshi Nagasaki[c] and Atsushi Ikeda *[a]

The development of boron agents with integrated functionality, including biocompatibility, high boron content, and cancer cell targeting, is desired to exploit the therapeutic efficacy of boron neutron capture therapy (BNCT). Here, we report the therapeutic efficacy of BNCT using a HER-2-targeted antibody-conjugated boron nitride nanotube/β-1,3-glucan complex. The anticancer effect of BNCT using our system was 30-fold that of the clinically available boron agent L-BPA/fructose complex.

Because of its high specificity, strong affinity, and excellent biocompatibility, antibody-conjugated drug delivery is one of the most promising modalities for cancer therapy.[1] To date, various types of antibodies, such as rituximab,[2] trastuzumab,[3] and cetuximab,[4] have been clinically developed and approved as pharmaceuticals by the Food and Drug Administration and the European Medicines Agency. A human epidermal growth factor receptor-2 (HER-2)-targeted antibody,[5] which modulates oncogenic signals by binding to this receptor, has been considered as an important biomarker for the development of tumor-targeted imaging and therapy for HER-2, which is overexpressed in a wide range of tumor types, including ovarian cancer, breast cancer, and prostate cancer.[6]

Recently, it was reported that antibody–drug complexes (ADCs), which are covalently modified with cytotoxic drugs (including monomethyl auristatin E,[7] monomethyl auristatin F,[8] and calicheamicin),[9] can cause the death of cancer cells selectively at low dose, which is achieved by binding to membrane proteins that are overexpressed in cancer cells, followed by the release of the pharmaceuticals after internalization. Despite these advantageous aspects for therapy, several issues remain regarding their delivery, including limited payload type, linker stability, and limited drug, which can cause the leakage of drugs, lessen their benefits, and cause heterogeneity of drug distribution.[10] From these points of view, the development of an invasive modality with high specificity is desired to exploit ADCs. More recently, photodynamic immunotherapy using antibody-conjugated photosensitizers allowed killing cancer cells without any harmful side effects.[11] Hence, the combination of ADCs with spatiotemporally controllable therapy is a powerful means to treat cancer.

Boron neutron capture therapy (BNCT) is one of the most elegant modalities in cancer therapy because of its non-invasiveness and efficient damage inducibility against the genomic DNA of the host cells.[12] BNCT is achieved *via* a nucleic reaction between ^{10}B and thermal and/or noncytotoxic epithermal neutron,[13] which generates cytotoxic α-lay and Li nuclei. The effective area of energy from these particles corresponds to the size of a cell (<10 μm), suggesting that BNCT enables the killing of cancer cells with high specificity if boron can accumulates in these cells selectively.[12] Currently, L-boronophenylalanine (L-BPA) and sodium borocaptate (BSH) are used as boron agents for BNCT in clinical settings.[14] Although these two boron agents exhibit excellent therapeutic efficacy, some issues remain regarding their delivery, including water solubility, tumor selectivity, and deliverability.[15] Therefore, the development of boron agents for BNCT is desired, to exploit the efficacy of this therapeutic modality.

In this study, we performed HER-2-targeted BNCT using a HER-2-targeting antibody conjugated to a boron nitride nanotube/β-1,3-glucan complex (BNNT/β-glucan complex) (Fig. 1). BNNTs have been expected to function as boron agents for BNCT because of their high boron density, thermal stability, chemical stability, and biocompatibility.[16] Despite these

[a]*Program of Applied Chemistry, Graduate School of Advanced Science and Engineering, 1-4-1 Kagamiyama, Higashi-Hiroshima City, 739-8527, Japan. E-mail: riku0528@hiroshima-u.ac.jp; aikeda@hiroshima-u.ac.jp*

[b]*Institute for Integrated Radiation and Nuclear Science, Kyoto University, 2, Asahiro-Nishi, Kumatori-cho, Sennan-gun, Osaka 590-0494, Japan*

[c]*Department of Applied Chemistry and Bioengineering, Graduate School of Engineering, Osaka Metropolitan University, 3-3-138 Sugimoto, Sumiyoshi-ku, Osaka City, 558-8585, Japan*

[d]*Program of Biotechnology, Graduate School of Integrated Sciences for Life, Hiroshima University, 1-3-1 Kagamiyama, Higashi-Hiroshima, 739-8530, Japan*

† Electronic supplementary information (ESI) available. See DOI: https://doi.org/10.1039/d3na00028a

‡ These authors contributed on this work equally.

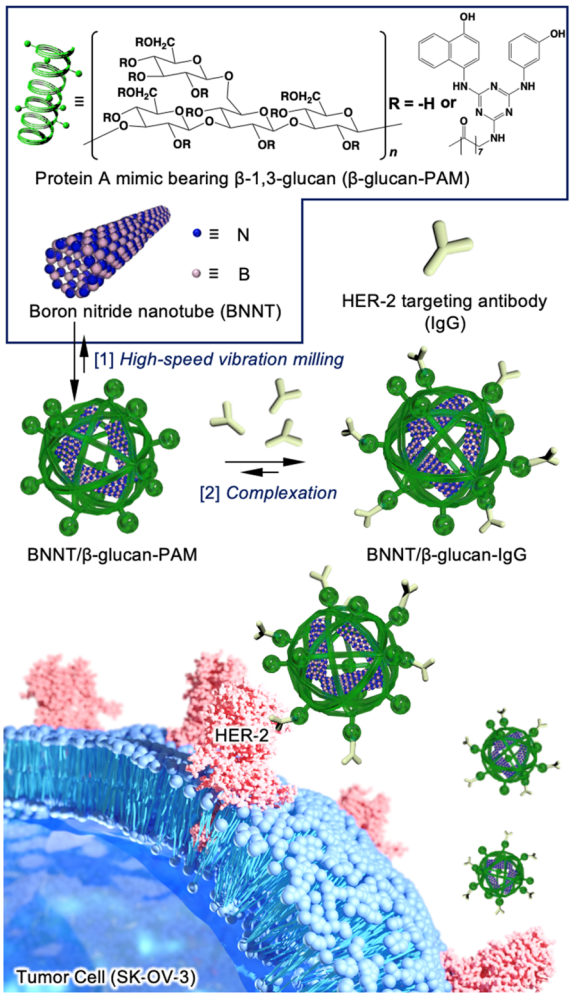

Fig. 1 Schematic illustration of the two-step method used to prepare the tumor-selective BNNT/β-glucan complex conjugated to a HER-2-targeting antibody (BNNT/β-glucan-IgG). [1] A boron nitride nanotube and a Protein A mimic bearing β-1,3-glucan (β-glucan-PAM) were complexed *via* the facile HSVM method. [2] The HER-2-targeting antibody was conjugated to BNNT/β-glucan using the binding ability of the Protein A mimic moiety.

fascinating properties, their biomedical application has remained limited because of their poor dispersibility in water and poor cancer selectivity.[17] We have developed water-solubilization techniques *via* a mechanochemical approach, *i.e.*, high-speed vibration milling (HSVM) using biomacromolecules, including cyclodextrins,[18] polysaccharides,[19,20] and polypeptides.[21] Cyclodextrin,[22] a β-glucan, and its derivative[23] have enabled the dissolution of carbon nanotubes, which are structural analogs of BNNTs. These advantageous characteristics encouraged us to develop a BNNT/β-glucan complex as a boron agent for BNCT.

As mechanochemical approach using ball milling can proceed undesirable chemical reaction to active species such as alkyne[24] and maleimide,[25] which have been conventionally used as conjugation unit with antibody, we employed a Protein A mimic molecule (PAM)[26] which can strongly bind to the Fc domain of an antibody *via* molecular recognition because of their relative robust structure. The PAM functionalized with carboxylic acid were synthesized (Scheme S1 and Fig. S1†) and the moiety was introduced to β-glucan *via* conventional condensation reaction (Scheme S2†). The ^{1}H NMR spectrum (dimethyl sulfoxide (DMSO)-d_6) of the resulting material (β-glucan-PAM) displayed several distinctive peaks, including the anomeric proton of β-glucan at 4.38 ppm and the phenyl proton of PAM at 8.20 ppm. The degree of substitution of the PAM coupled to β-glucan per 100 glucose units was quantitatively determined to be 11.1 based on the integrated areas of the signals of the glucopyranose rings (4.38 ppm) and PAM (8.20 ppm), respectively (Fig. S2†). The BNNT/β-glucan complex and BNNT/β-glucan-PAM complex were prepared *via* HSVM as reported previously.[20] We confirmed the dispersibility of BNNT in water by measuring the boron concentration using inductivity-coupled plasma-atomic emission spectroscopy (ICP-AES). As a result, β-glucan afforded dissolution of BNNT at 544 ppm (Table 1). The boron concentration in the system was a level that is applicable as a boron agent for BNCT. We further measured the hydrodynamic diameter (D_{hy}) of these complexes. Dynamic light scattering measurements revealed that the D_{hy} of the BNNT/β-glucan complex and BNNT/β-glucan-PAM complex was 100 and 80 nm, respectively. The sizes of the complex corresponded to the passive tumor targeting property, *i.e.*, enhanced permeability and retention effect.[27] Transmission electron microscopy (TEM) revealed that the BNNT/β-glucan complex are rod like morphology (Fig. 2a) and the length of BNNT got shortened *via* HSVM (Fig. S3†). In addition, the bundle-like structure of the complexes was observed by transmission electron microscopy (TEM) (Fig. S3†). In general, robust one-dimensional materials such as BNNT and CNT can be cleaved by mechanical stress such as ultrasonic.[28] The mechanochemical forces with ball milling can also cleave BNNT. The ζ-potential of the complexes was electrically neutral because of the character of the backbone of β-glucan.

Next, we performed antibody conjugation with the BNNT/β-glucan-PAM complex. Complexation with the antibody was confirmed by fluorescence resonance energy transfer (FRET) using fluorescently labeled β-glucan-PAM.[29] FRET is observed only when two fluorophores are closely located (<2 nm). FRET was observable in the current condition (Fig. 2b), and energy transfer occurred more efficiently as the amount of FITC-labeled antibody increased. This result indicates that the antibody was successfully introduced into the complex (BNNT/β-glucan-IgG complex). In addition, the size and ζ-potential of the complex did not change significantly during the conjugation

Table 1 Solution properties of BNNT/β-glucan complexes[a]

	Boron/ppm	D_{hy}/nm	PDI	ζ-Potential/mV
BNNT/β-glucan	544	99.0 ± 0.5	0.16	−13.0 ± 0.9
BNNT/β-glucan-PAM	—	80 ± 5	0.30	−7.7 ± 0.9
BNNT/β-glucan-IgG	—	130 ± 7	0.17	−6.0 ± 3.0

[a] Dynamic light scattering measurement was carried out at 25 °C in MilliQ (pH, 7.4) and PDI value was calculated by cumulant method. ζ-Potential was measured by using a capillary cell.

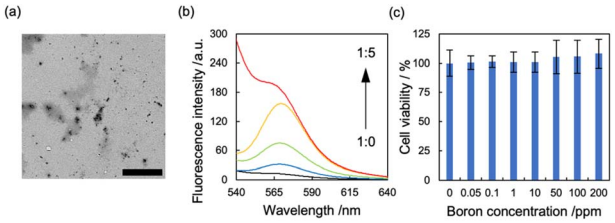

Fig. 2 Characteristics of BNNT/β-glucan complexes and their interactions with IgG. (a) TEM image of BNNT/β-glucan. Scale bar = 1 μm. (b) Complexation between BNNT/β-glucan-PAM and IgG, which was estimated by the upregulation of rhodamine B-labeled BNNT/β-glucan-PAM fluorescence in the presence of FITC-labeled IgG. The molar ratios of BNNT/β-glucan-PAM to IgG were 1 : 0, 1 : 2, 1 : 3, 1 : 4, and 1 : 5. The excitation and emission wavelengths were λ_{em} = 495 nm and λ_{em} = 540–640 nm, respectively. (c) Cell viability of normal cells (L929) treated with the BNNT/β-glucan complex.

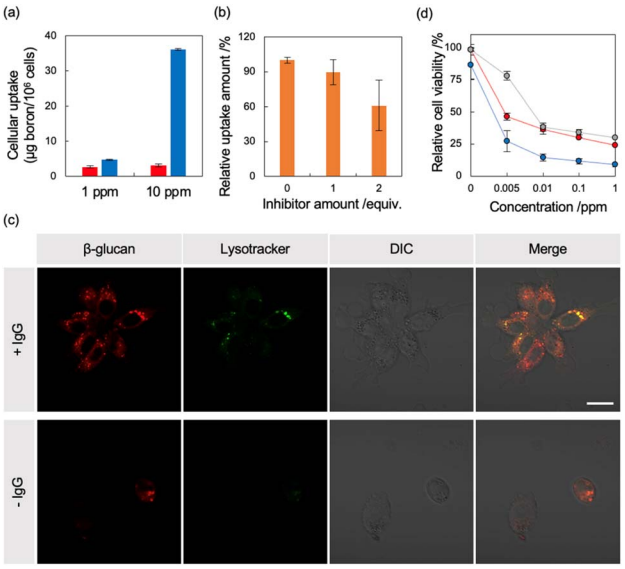

Fig. 3 Evaluation of the BNNT/β-glucan-IgG complex as a tumor-selective boron agent for BNCT. (a) Intracellular uptake of BNNT into SK-OV-3 cells in the presence (blue) and absence (red) of IgG. The cells were exposed to the samples ([B] = 1, 10 ppm) for 24 h. (b) Intracellular uptake mechanism of the BNNT/β-glucan-IgG complex. SK-OV-3 cells were preincubated with Free HER-2-targeting antibody, as the inhibitor. The cellular uptake of BNNT was compared with that observed in cells treated without Free HER-2-targeting antibody. (c) Subcellular distribution of the BNNT/β-glucan complex and BNNT/β-glucan-IgG complex in SK-OV-3 cells, as observed using confocal laser scanning microscopy. After 24 h of incubation with the BNNT/β-glucan-IgG complex and BNNT/β-glucan complex (red), lysosomes were stained with Lysotracker Green (green). Scale bar = 20 μm. (d) Efficacy of BNCT regarding cell viability in SK-OV-3 cells. The cells were incubated with the BNNT/β-glucan-IgG complex (blue), BNNT/β-glucan complex (red), or BPA-fructose (gray) for 24 h. After incubation, the cells were exposed to thermal neutron irradiation with a fluence of 6.3×10^{11} n cm^{-2}. The cell viabilities were evaluated after additional incubation for 24 h.

process (Table 1). To determine the colloidal stability of BNNT/β-glucan-IgG complex in physiological conditions (PBS; pH, 7.4; 37 °C), the size of the complex and the boron concentration of the dispersion were measured at each time point (0, 24, 48, and 72 h). There are no significant changes in D_{hy} of the complex and boron concentration in initial 24 h, however secondary aggregation of the complex and undesirable precipitation was found with time after 48 h incubation, resulting in the size of complex gradually increased and the boron concentration got decreased (Fig. S4†).

We examined the applicability of the BNNT/β-glucan complex as a boron carrier by measuring the viability of murine fibroblast cells (L929) in the absence of thermal and/or epithermal neutrons using a modified MTT assay. No apparent cytotoxicity against the normal cell line was observed, even at the highest concentration (Fig. 2c), suggesting that our system based on polysaccharides is a nontoxic boron carrier. As the accumulation of boron agents within cells is critical in BNCT, next we evaluated the deliverability of the boron agent into human ovarian cancer cells (SK-OV-3),[30] which overexpress HER-2, by quantifying the intracellular boron concentration *via* ICP-AES. Using BNNT/β-glucan without the antibody targeting HER-2, the cellular uptake of boron was 3.1 μg/1.0×10^5 cells. In contrast, conjugation with an antibody targeting HER-2 enhanced cellular uptake of BNNT into SK-OV-3 cells by 12-fold (37.0 μg/1.0×10^5 cells) (Fig. 3a). Furthermore, the addition of a HER-2-targeting IgG to cells inhibited the accumulation of the BNNT/β-glucan-IgG complex in SK-OV-3 cells (Fig. 3b), indicating that the cellular uptake of BNNT/β-glucan complex is achieved *via* HER-2-targeting antibody-mediated endocytosis, as expected. Taken together, these results suggest that the BNNT/β-glucan-IgG complex works as a HER-2-targeting boron carrier for BNCT.[31]

As the subcellular distribution of the boron agents is also significant in BNCT, in addition to the amount of cellular uptake, observation of the treated cells using confocal laser scanning microscopy was performed to visualize the subcellular distribution of the agents. To determine whether the cellular uptake of the complex is dominantly achieved *via* endocytosis, we visualized lysosomes using a commercially available fluorophore, Lysotracker Green. As shown in Fig. 3c, in SK-OV-3 cells, stronger fluorescence signals from rhodamine B-labeled β-glucan were detected within cells in the case of the BNNT/β-glucan-IgG complex compared with the BNNT/β-glucan complex (Fig. 3c). In addition, a large proportion of the fluorescent signals from the delivered complex overlapped with the fluorescent signals from lysosomes, indicating that the BNNT/β-glucan complex internalizes into cells mainly *via* endocytosis. As shown in Fig. S5,† the fluorescent signals from Rh B were decreased by pretreatment with a HER-2-targeting IgG, which is a competitive inhibitory condition; these trends were comparable to those observed using the cellular uptake studies.

We next evaluated the therapeutic efficacy of BNCT regarding cell viability using the BNNT/β-glucan complex and the BNNT/β-glucan-IgG complex against SK-OV-3 cells. Here, we employed the clinically available boron agent, L-BPA/fructose complex, as a comparison. After exposure to the boron agents for 24 h, the cells were exposed to thermal and/or epithermal neutrons at 1 MW for 70 min (fluence, 6.3×10^{11} n cm^{-2}). In

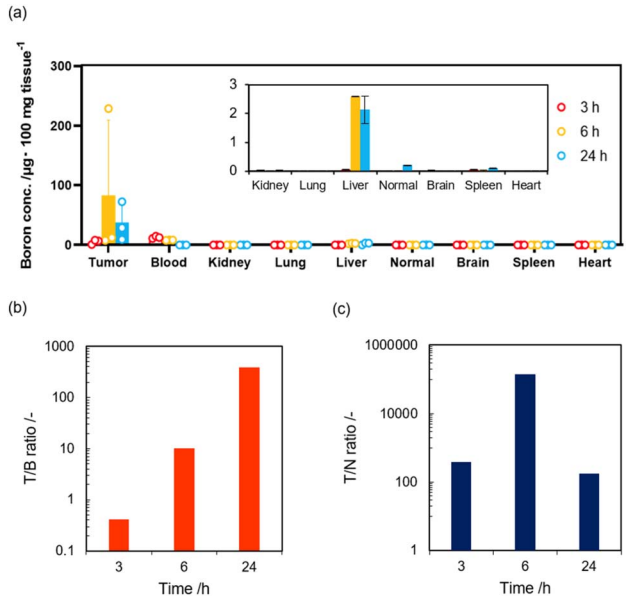

Fig. 4 Pharmacokinetics of BNNT/β-glucan-IgG complex in SK-OV3 xenograft model mice. (a) Biodistribution of the BNNT/β-glucan-IgG complex. The inset represents magnified graph for the accumulation in kidney, lung, liver, normal, brain, spleen and heart. Tumor-bearing mice were established through subcutaneous injection of a SK-OV-3 cell suspension at the right femur of nude mice. After 30 days incubation, the BNNT/β-glucan-IgG complex ([B] = 200 ppm, mice 100 μL) were intravenously injected. At 3, 6 and 24 h post injection, tumors, blood, and organs (kidney, lung, liver normal (skin), brain, spleen, and heart) were collected and lysed by aqua regia. The resulting solution was analyzed using ICP-AES (n = 3). Data represents mean ± SD and individual measurements. (b) The ratio of boron concentration in tumor tissue against blood. (c) The ratio of boron concentration in tumor tissue against normal tissue.

absence of thermal and/or epithermal neutron irradiation, no apparent cytotoxicity was found (Fig. S6†). In contrast, thermal and/or epithermal neutron irradiation induced the death of the cells treated with boron agents according to boron concentration (Fig. 3d). The half-maximal inhibitory concentration (IC_{50}) of the L-BPA/fructose complex, BNNT/β-glucan complex, and BNNT/β-glucan-IgG complex was determined to be 87, 4.6, and 3.0 ppb, respectively. These results indicate that the BNNT/β-glucan complex improved thermal-neutron-induced cytotoxicity compared with the clinically available boron agent, L-BPA/fructose complex. Moreover, conjugation with a HER-2-targeting antibody boosted the therapeutic efficacy of the BNNT/β-glucan complex, as expected. Similar trends in cytotoxicity were found at 48 h (Fig. S7†). These results suggest that our systems are applicable as boron agents and that the BNNT/β-glucan-IgG complex can work as HER-2-targeting boron agent for BNCT.

Finally, we investigated the *in vivo* delivery of BNNT/β-glucan-IgG complex toward tumor xenograft model mice to confirm their potential for BNCT. SK-OV3 xenograft mice were prepared by subcutaneous injection of SK-OV3 cells to Balb/c nu/nu (male, 4 weeks old, 18 g).[32] When tumor grew to approximately 50 mm^3, BNNT/β-glucan-IgG complex was intravenously administered to the mice (200 ppm, 100 μL). At each time point (3, 6, and 24 h), organs (tumor, blood, heart, lung, liver, kidney, spleen, and skin) were isolated to quantify accumulation of BNNT. As a result, current systems are more likely to accumulate in tumor tissue and the concentration of boron agents in tumor tissues reached up to 36.8 μg × 100 mg^{-1} at 24 h-post injection (Fig. 4a). We further estimated tumor selectivity by comparing the accumulation amount of boron agent in tumor tissue with blood (T/B ratio) or skin employed as normal tissue (T/N ratio). At 24 h-post injection, T/B ratio and T/N ratio were calculated to be 390 and 170, respectively, which meet clinical demands (>2.5) (Fig. 4b and c).[33] These results clearly indicate that the BNNT/β-glucan-IgG complex worked as a HER-2 targeted boron agent for BNCT.

In summary, we reported the efficient delivery of a boron agent into HER-2-positive cells using the BNNT/β-glucan complex modified with an antibody targeting HER-2. The excellent deliverability of our system resulted in the boosting of BNCT efficacy, with an effect on cell viability that was stronger than that of the clinically available boron agent, L-BPA/fructose complex. Moreover, the high selective tumor accumulation of the BNNT/β-glucan-IgG complex was also confirmed exceeding the requirements of clinical use. These results suggest that the BNNT/β-glucan-IgG complex has a promising potential as a boron agent for BNCT for cancer.

Author contributions

All authors discussed the results and contributed to the final manuscripts. R. K., K. K., and K. Y. are mainly conducted all the examinations. R. K., Y. K., H. H., Y. S., K. B., A. T., K. Y., Y. M., H. A., T. T., Y. S., K. T., T. N., carried out irradiation studies. R. K., T. N., and A. I. designed experiments. R. K., K. Y. and A. I. wrote the manuscript. T. K. and S. K. analysed the results from animal experiments.

Conflicts of interest

There are no conflicts to declare.

Acknowledgements

This research was financially supported by JSPS KAKENHI, Grant-in-Aid for Young Scientists (R. K., 19K15401; JP22K18196), Grant-in-Aid for Scientific Research B (T. N.; 19H04472), JST A-STEP (R. K., JPMJTM20RC), JST ACT-X (R. K., JPMJAX2225) and MEXT Research Fellowship (K. Y.). TEM and CLSM experiments were conducted in N-BARD in Hiroshima University. All animal experiments were approved by ethics committee for animal welfare of Hiroshima University (accreditation no. C22-43).

Notes and references

1 A. L. Nelson, E. Dhimolea and J. M. Reichert, *Nat. Rev. Drug Discovery*, 2010, **9**, 767–774.

2 A. D. Salama and C. D. Pusey, *Nat. Clin. Pract. Nephrol.*, 2006, **2**, 221–230.
3 R. Nahta and F. J. Esteva, *Oncogene*, 2007, **26**, 3637–3643.
4 P. Kirkpatrick, J. Graham and M. Muhsin, *Nat. Rev. Drug Discovery*, 2004, **3**, 549–550.
5 A. P. Meert, B. Martin, M. Paesmans, T. Berghmans, C. Mascaux, J. M. Verdebout, P. Delmotte, J. J. Lafitte, J. P. Sculier and J. P. Sculier, *Br. J. Cancer*, 2003, **89**, 959–965.
6 D. Y. Oh and Y. J. Bang, *Nat. Rev. Clin. Oncol.*, 2020, **17**, 33–48.
7 R. L. Best, N. E. LaPointe, O. Azarenko, H. Miller, C. Genualdi, S. Chih, B. Q. Shen, M. A. Jordan, L. Wilson, S. C. Feinstein and N. J. Stagg, *Toxicol. Appl. Pharmacol.*, 2021, **421**, 115534.
8 S. O. Doroina, B. A. Mendelsohn, T. D. Bovee, C. G. Cerveny, S. C. Alley, D. L. Meyer, E. Oflazoglu, B. E. Toki, R. J. Sanderson, R. F. Zabinski, A. F. Wahl and P. D. Senter, *Bioconjugate Chem.*, 2006, **17**, 114–124.
9 A. D. Ricart, *Clin. Cancer Res.*, 2011, **17**, 6417–6527.
10 A. Beck, L. Goetsch, C. Dumontet and N. Corvaia, *Nat. Rev. Drug Discovery*, 2017, **16**, 315–337.
11 H. Kobayashi and P. L. Choyke, *Acc. Chem. Res.*, 2019, **52**, 2332–2339.
12 R. F. Barth, A. H. Soloway, R. G. Farichild and R. M. Brugger, *Cancer*, 1992, **70**, 2995–3007.
13 J. A. Coderre and G. M. Morris, *Radiat. Res.*, 1999, **7**, 1–18.
14 K. Hu, Z. Yang, L. Zhang, L. Xie, L. Wang, H. Xu, L. Josephson, S. H. Liang and M. R. Zhang, *Coord. Chem. Rev.*, 2020, **15**, 213139.
15 R. F. Barth, P. Mi and W. Yang, *Cancer Commun.*, 2018, **38**, 35.
16 C. S. T. Castillo, C. Bruel and J. R. Tavares, *Nanoscale Adv.*, 2020, **2**, 2497–2506.
17 H. Nakamura, H. Koganei, T. Miyoshi, Y. Sakurai, K. Ono and M. Suzuki, *Bioorg. Med. Chem. Lett.*, 2015, **25**, 172–174.
18 T. Yumoto, S. Satake, S. Hino, K. Sugikawa, R. Kawasaki and A. Ikeda, *Org. Biomol. Chem.*, 2020, **18**, 6702–6709.
19 R. Kawasaki, K. Yamana, R. Shimada, K. Sugikawa and A. Ikeda, *ACS Omega*, 2021, **6**, 3209–3217.
20 K. Yamana, R. Kawasaki, Y. Sanada, A. Tabata, K. Bando, K. Yoshikawa, H. Azuma, Y. Sakurai, S. Masunaga, M. Suzuki, K. Sugikawa, T. Nagasaki and A. Ikeda, *Biochem. Biophys. Res. Commun.*, 2021, **559**, 210–216.
21 R. Kawasaki, S. Kawamura, S. Hino, K. Yamana and A. Ikeda, *Adv. Mater.*, 2022, **3**, 467–473.
22 A. Ikeda, K. Hayashi, T. Konishi and J. Kikuchi, *Chem. Commun.*, 2004, **11**, 1334–1335.
23 M. Numata, M. Asai, K. Kaneko, S. H. Bae, T. Hasegawa, K. Sakurai and S. Shinkai, *J. Am. Chem. Soc.*, 2005, **127**, 5875–5884.
24 Y. Guo, C. Feng, K. Kubota and H. Ito, *Chem. Sci.*, 2022, **13**, 430–438.
25 Z. Wang and S. L. Craig, *Chem. Commun.*, 2019, **55**, 12263–12266.
26 K. Nishimori, M. Maruyama, Y. Shimazaki, M. Ouchi and M. Sawamoto, *ACS Appl. Polym. Mater.*, 2019, **1**, 1925–1929.
27 H. Maeda, J. Wu, T. Sawa, Y. Matsumura and K. Hori, *J. Contr. Release*, 2000, **65**, 271–284.
28 G. Ciofani, S. Danti, G. G. Genchi, B. Mazzolai and V. Mattoli, *Small*, 2013, **9**, 1672–1685.
29 H. Ayame, N. Morimoto and K. Akiyoshi, *Bioconjugate Chem.*, 2008, **19**, 882–890.
30 V. A. Gall, A. V. Philips, N. Qiao, K. C. Dwyer, A. A. Perakis, M. Zhang, G. T. Clifton, P. Sukhumalchandra, Q. Ma, S. M. Reddy, D. Yu, J. J. Molldrem, G. E. Peoples, G. Alatrash and E. A. Mittendorf, *Cancer Res.*, 2017, **77**, 5374–5383.
31 M. Iijima, H. Kadoya, S. Hatahira, S. Hiramatsu, G. Jung, A. Martin, J. Quinn, J. Jung, S. Y. Jeong, E. K. Choi, T. Arakawa, F. Hinako, M. Kusunoki, N. Yoshimoto, T. Niimi, K. Tanizawa and S. Kuroda, *Biomaterials*, 2011, **32**, 1455–1464.
32 K. Ito, S. Hamamichi, M. Asano, Y. Hori, J. Matsui, M. Iwata, Y. Funahashi, K. O. Umeda and H. Fujii, *Cancer Sci.*, 2015, **107**, 60–67.
33 R. Kawasaki, H. Hirano, K. Yamana, H. Isozaki, S. Kawamura, Y. Sanada, K. Bando, A. Tabata, K. Yoshikawa, H. Azuma, T. Takata, H. Tanaka, Y. Sakurai, M. Suzuki, N. Tarutani, K. Katagiri, S. Sawada, Y. Sasaki, K. Akiyoshi, T. Nagasaki and A. Ikeda, *Nanomed. Nanotechnol. Biol. Med.*, 2023, **49**, 102659.